Influences of grain size and salinity on pressure-temperature thresholds for methane hydrate stability in JAPEX/JNOC/GSC Mallik 2L-38 gas hydrate research-well sediments

J.F. Wright[1], S.R. Dallimore[1], and F.M. Nixon[1]

Wright, J.F., Dallimore, S.R., and Nixon, F.M., 1999: Influences of grain size and salinity on pressure-temperature thresholds for methane hydrate stability in JAPEX/JNOC/GSC Mallik 2L-38 gas hydrate research-well sediments; in *Scientific Results from JAPEX/JNOC/GSC Mallik 2L-38 Gas Hydrate Research Well, Mackenzie Delta, Northwest Territories, Canada, (ed.) S.R. Dallimore, T. Uchida, and T.S. Collett; Geological Survey of Canada, Bulletin 544, p. 229–240.*

Abstract: This paper summarizes laboratory determinations of the pressure-temperature (P-T) phase equilibrium conditions for methane hydrate stability in sediments recovered from the gas-hydrate-bearing interval at JAPEX/JNOC/GSC Mallik 2L-38 gas hydrate research well. Three test samples consisted of quartz-rich sand with in situ pore-water salinities of 4 ppt (parts per thousand), 20 ppt, and 40 ppt. A fourth sample was dominated by silt, with a salinity of 31 ppt. Initially, methane hydrate was regrown in the sediments, followed by the determination of P-T stability thresholds between 0°C and 12°C. Comparisons with published data for methane hydrate stability in pure gas-water systems indicate no appreciable shift in P-T stability conditions in sand with salinity of 4 ppt, but suggest a progressively increasing shift towards the higher pressure, lower temperature region for sand samples with elevated salinity. Test results for the saline silt sample indicate an additional shift in the stability threshold attributed to the effect of the porous medium in fine-grained sediments.

Résumé : Le présent document expose sommairement les déterminations effectuées en laboratoire des conditions d'équilibre des phases en fonction de la pression et de la température (P-T) assurant la stabilité des hydrates de méthane contenus dans les sédiments prélevés dans l'intervalle à hydrates de gaz dans le puits de recherche sur les hydrates de gaz JAPEX/JNOC/GSC Mallik 2L-38. Les trois échantillons d'essais étaient composés de sable riche en quartz dont l'eau interstitielle montrait des salinités en place de 4×10^{-3}, de 20×10^{-3} et de 40×10^{-3}. Un quatrième échantillon, formé essentiellement de silt, présentait une salinité de 31×10^{-3}. Au départ, on a reproduit de l'hydrate de méthane dans les sédiments, puis on a déterminé des seuils de stabilité en fonction de la pression et de la température entre 0 et 12 °C. Les comparaisons effectuées avec des données publiées sur la stabilité de l'hydrate de méthane dans les systèmes à gaz et eau purs ne montrent pas de changement sensible dans le seuil de stabilité de l'hydrate de méthane en fonction de la pression et de la température dans le sable dont la salinité est de 4×10^{-3}, mais permettent de supposer qu'un changement de plus en plus important s'effectue progressivement dans les échantillons de sable à forte salinité, vers la région où la pression est plus élevée et la température plus basse. Les résultats des essais réalisés sur l'échantillon de silt salin indiquent que le seuil de stabilité s'est encore modifié en raison de l'incidence du milieu poreux dans les sédiments à grain fin.

[1] Geological Survey of Canada, 601 Booth Street, Ottawa, Ontario, Canada K1A 0E8

INTRODUCTION

In recent years a number of research projects have investigated marine occurrences of gas hydrate, with extensive drilling and geophysical studies supported by the Ocean Drilling Program. Gas hydrate studies in permafrost regions have generally been more limited, and typically rely on data collected during conventional hydrocarbon exploration drilling (Judge and Majorowicz, 1992; Yakushev and Collett, 1992; Collett, 1993). North America's first well documented gas hydrate samples were recovered from permafrost-bearing sediments in the Mackenzie Delta, Northwest Territories (Dallimore and Collett, 1995; Dallimore and Collett, 1998). In this case, core samples from a 451 m corehole contained gas hydrate as visible lenses as well as in dispersed form within sediment pore spaces. In 1998, the 1150 m JAPEX/JNOC/GSC Mallik 2L-38 gas hydrate research well was drilled in the Mackenzie Delta, Northwest Territories, Canada as part of a collaborative research agreement between the Geological Survey of Canada (GSC) and the Japanese National Oil Corporation (JNOC). Core samples recovered from subpermafrost gas-hydrate-bearing intervals between 897–952 m are being extensively studied as part of a major scientific research program, subsequent to fieldwork, being co-ordinated by the GSC (Dallimore et al., 1999).

Gas hydrate observed in Mallik 2L-38 core samples was primarily within the sediment pore spaces with rare visible gas hydrate. As discussed in a number of papers in this volume, a suite of qualitative and quantitative indicators suggest that at Mallik 2L-38 in situ gas hydrate saturation values (pore occupancy) vary between 20% and 80%. The highest gas hydrate concentrations observed in core samples occurred in medium- to fine-grained sands and gravely sands. Given the difficulty in recovering natural core samples at in situ pressures and temperatures, laboratory experiments provide an opportunity to investigate the characteristics of gas hydrate in porous sediments under controlled environmental conditions. This paper describes an experimental test program that determined the methane hydrate pressure-temperature stability field for a variety of gas-hydrate-bearing sediments from the Mallik 2L-38 well. The kinetics and heat transfer characteristics of gas hydrate formation in a Mallik 2L-38 test sample are discussed with reference to a plot of the pressure-temperature history during the initial cycle of gas hydrate formation. The relevance of laboratory measurements to the natural occurrence of gas hydrate in a geological setting is also discussed.

MATERIALS AND METHODS

GSC test cell

A new gas hydrate test cell, developed by the GSC to study gas hydrate formation and dissociation in porous media (Wright et al., 1999), was utilized for the current suite of laboratory tests (Fig. 1). The test cell, based on an original Russian design (Ershov and Yakushev, 1992), features precision thermistors and pressure transducers that continuously monitor

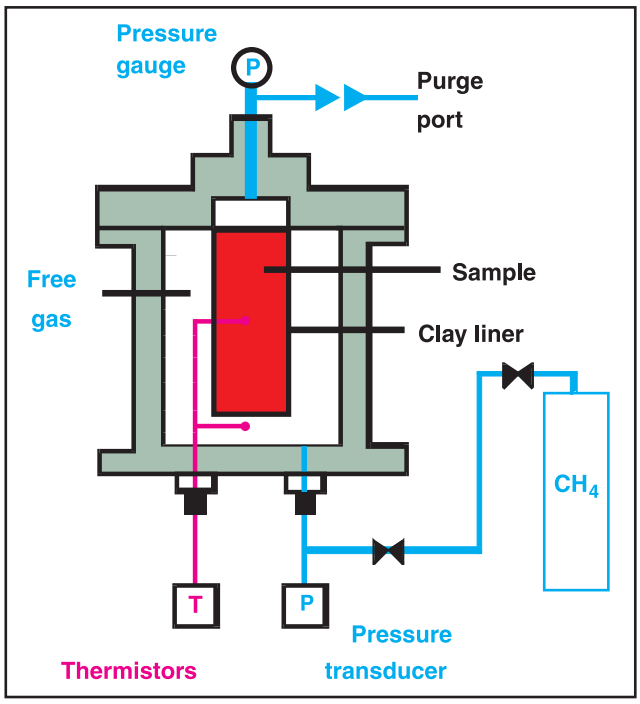

Figure 1. *Conceptual diagram of the GSC gas hydrate test cell.*

pressure-temperature (P-T) conditions within the cell and sediment samples. Recorded P-T histories provide insight into the kinetics of natural gas hydrate formation and dissociation, including heat transfer characteristics, rates of gas consumption and release, and P-T equilibrium thresholds. The test cell accommodates either of two sample holders with different sample capacities (about 102 cm^3 and 140 cm^3, each about 9 cm in length). The interior free-gas volume of the cell is about 270–290 cm^3 depending on sample characteristics and the sample holder used.

Sediment characteristics

The sedimentology of the main cored interval (886–952.6 m) (all depths measured from kelly bushing [8.31 m above sea level]) has been described by others (Jenner et al., 1999), as have the methods for estimating the in situ gas hydrate concentrations (Miyairi et al., 1999). In summary, the highest gas hydrate concentrations were observed within unconsolidated sands and silty sands occurring between 896 m and 926 m. Although the grain size and mineralogy of the sands were relatively constant within these sediments, pore-water salinity varied from 0–60 ppt and in situ pore occupancy by gas hydrate ranged from 30% to more than 80%. In general, higher pore-water salinities were correlated with lower gas hydrate concentrations (Winters et al., 1999). When retrieved at the surface, sand samples were typically frozen (-2.3°C to -3°C) and contained pore space gas hydrate in variable concentrations, with occasional visible forms of gas hydrate observed (Uchida et al., 1999). Although there was no visible evidence of gas hydrate within silt-dominated sediments immediately above and below this

Table 1. Summary of test sample characteristics.

Sample #	Depth (m)	Class	Remoulded dry density (g/cm^3)	Gravimetric water content (%)	Water saturation (%)	Salinity (ppt)	Silt (%)	In situ GH%*
1	898.4	Sand	~1.6	15.5	62	4	4–6	70
2	922.1	Sand	~1.6	17.4	69	20	4	20–40
3	893.6	Sand	~1.6	~17	66	40	n/a	< 10
4	938.2	Silt	~1.5	15.3	54	31	87	< 20**

* Gas hydrate saturation (pore occupancy) estimated from well logs
** Tendency for over-estimation in silts (Collett et al., 1999)
n/a= not available

major gas-hydrate-bearing interval (and core temperatures were greater than 0°C when recovered), analysis of well logs suggest in situ gas hydrate saturations between 0 and 15%. Field tests on samples from the cored interval indicate gravimetric water contents between 16% and 22% (Winters et al., 1999). Derived sediment porosities by core parameters and well-log estimates ranged from 30% to 40%. Gas devolved from core in this interval consisted of greater than 99% methane with a C1/(C2+C3) ratio of about 500 (Lorenson et al., 1999). While this information does not provide definitive evidence for the genetic origin of the gas-hydrate-forming gases, it supports our assumption that Structure I methane hydrate dominates at Mallik 2L-38.

Four representative samples, collected from cores recovered between 893.6 m and 938.2 m depth, were tested in the experiments described in this paper (Table 1). Three of the samples were dominated by sand, and were taken from cores with varied pore-water salinities and in situ gas hydrate concentrations. The sands were well sorted and consisted of approximately 95% sand-size particles (with 50% of grains between 0.25 and 0.35 mm) and less than 3% silt. Sand grains were angular to subrounded (Fig. 2), and dominated by quartz (55%) and amphibole (40%). The pore-water salinity of sample 1 was low (4 ppt) with an in situ gas hydrate concentration exceeding 70%. Sample 2 was of intermediate salinity (20 ppt) with gas hydrate concentrations between 20% and 40%. Sample 3 was highly saline (40 ppt) with less than 10% of pore space occupied by gas hydrate. Finally, a silt sample, taken from the lower portion of the cored interval (sample 4), had a pore-water salinity of 31 ppt, and gas hydrate concentrations below 20%. Grain-size analysis indicated a silt fraction of approximately 87%, with about 10% sand.

Following initial core recovery in the field, test samples were maintained in the frozen state until immediately before placement in the test cell. After thawing, the water content of sample 1 (898.40 m) was approximately 15.5%, indicating a minor loss of water relative to in situ conditions (*see* Winters et al., 1999). Remolding and compaction of the sample yielded a dry density of about 1.6 g/mL with approximately 60% water saturation. No additional water was added during preparation of the samples, in order to maintain the approximate in situ pore-water salinity.

Figure 2. *Photomicrograph of a Mallik 2L-38 test sand (30x).*

Test procedures

Gas hydrate testing for each sample was carried out in two stages. In stage I methane hydrate was regrown in the test sediments. Stage II involved the determination of the pressure-temperature thresholds for methane hydrate stability between 0°C and 12°C. The recorded pressure-temperature (P-T) history and cumulative methane consumption during a complete cycle of methane hydrate formation, subsequent freezing and thawing, and dissociation of hydrate for Mallik 2L-38 sample 2 is presented in Figure 3. This plot is representative of the data stream acquired during each experiment except that the magnitude and duration of the various heat exchanges between the cell and sample varied between the different test samples.

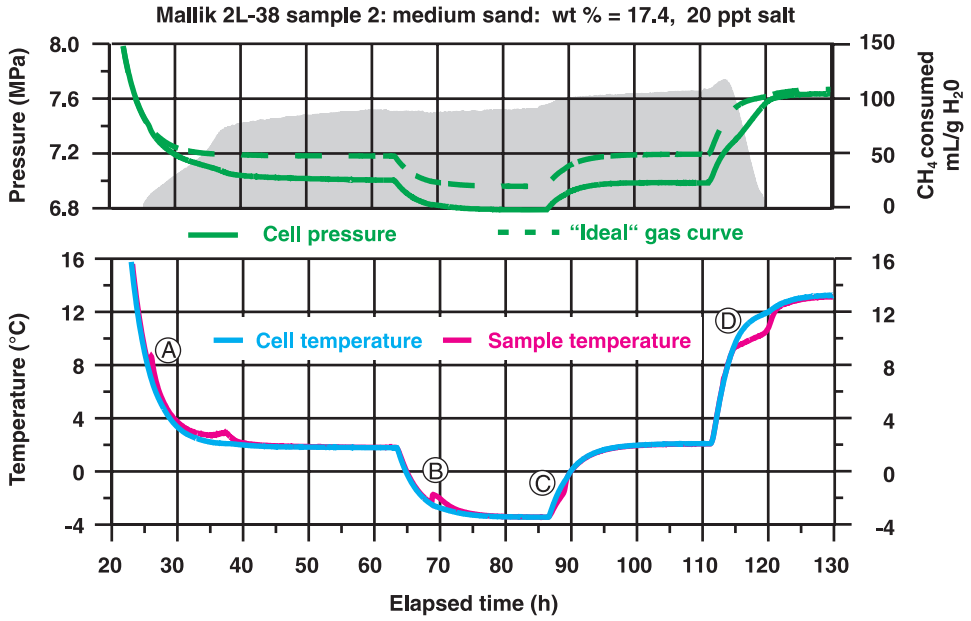

Figure 3. *Pressure-temperature history of the initial cycle of methane (CH_4) hydrate formation in Mallik 2L-38 sand (sample 2) with a pore-water salt concentration of 20 ppt, wt %= gravimetric water content.*

A) *During initial system cooling, cell pressure decreased in accordance with the general gas laws (PVT=P'V'T') permitting determination of the expected pressure response to changing temperatures (dashed pressure curve) in Figure 3. Beyond point 'A', the decrease in cell was greater than could be accounted for by temperature changes alone, and the excess was assumed to be due to the incorporation of CH_4 gas into gas hydrate. A coincident increase in sample temperature at 'A' is interpreted as the release of reaction heat during gas hydrate formation. Growth of gas hydrate was vigorous during the next 15 hours, as indicated by the slope of the CH_4 consumption curve (shaded area), and was accompanied by a sharp increase in sample temperature relative to that of the cell which persisted throughout the period of rapid growth. During the next 20 hours (h 40–60) a reduced rate of CH_4 consumption was observed, with a further reduction to very low values beyond hour 60 (<0.1 mL/h/g). The amount of gas hydrate formed is expressed as the equivalent volume of CH_4 consumed (incorporated per gram of soil water). Theoretically, complete integration of 1 g of water into Structure I hydrate consumes approximately 205 mL of methane gas.*

B) *A freezing cycle was initiated at about hour 64. At 'B' sample temperature increased sharply, but without a coincident drop in cell pressure as was observed at 'A'. This was interpreted as a release of latent heat during freezing of the remaining soil pore water. Significant subcooling, and a freezing-point depression of nearly 2°C is evident (attributed to the elevated pressure and pore-water salinity). The release of latent heat persisted strongly for 2–3 hours, indicating that considerable amounts of free water remained within the sample prior to the freezing event. Initially, a modest reduction in total CH_4 consumption accompanied the addition of fusion heat, followed by a resumption of low consumption rates during the remainder of the freezing period (between hours 70–87).*

C) *Following thawing of the sample at 'C', ice formed at 'B' began to melt, absorbing heat from the surrounding sediment matrix, and reducing sample temperature relative to that of the cell. Methane consumption resumed at an elevated rate for a short period of time. This increase in the rate of CH_4 consumption may be related to the so-called water memory effect, in which a large number of hydrogen bonds persist in liquid water for some time following melting of ice (Makagon, 1981). It has been speculated that such water may be more readily integrated into the gas hydrate lattice structure than ordinary water. Total methane consumed at the termination of stage I was approximately 115 mL/g of water, or about 56% of the theoretical maximum. The estimated total volume of methane incorporated into pore space gas hydrate was about 4.03 litres (115 mL/g H_2O x 35 g).*

D) *Upon warming of the test cell, CH_4 gas hydrate began to dissociate at 'D'. The endothermy of hydrate dissociation within sediment pores absorbs heat from the surrounding soil matrix and causes an abrupt deviation of sample temperature from the established warming trend. Pressure-temperature conditions at the point of deviation mark the P-T stability threshold for methane hydrate in the test sediment. Hydrate dissociation in sediments is typically more rapid than hydrate formation, with complete dissociation accomplished within 5–6 hours in this example.*

Stage I: regrowth of methane hydrate in Mallik 2L-38 sands

Following loading of the remolded sample into the test cell, methane gas (>99.997 % pure) was introduced at just above atmospheric pressure and allowed to flow through the cell for sufficient time to purge it of air (about 30–40 min). The cell was then hermetically sealed and the internal pressure was gradually increased to the initial working pressure (typically 7–10 MPa). Subsequent cooling of the cell (to a temperature of 0–5°C) established a P-T condition well within the zone for methane hydrate stability, thereby promoting the formation of methane hydrate within the sediments. The pressure and temperature of the free-gas volume within the test cell, and the temperature of the interior of the soil sample, were continuously recorded throughout the experiments.

Stage II: determining P-T stability thresholds

Sample 1 — Sand with 4 ppt salt

The growth phase of sample 1 produced a relatively large amount of gas hydrate, allowing for controlled dissociation over an extended range of temperatures. Following initial gas hydrate formation, the system was further cooled to approximately -7°C in order to stabilize the sample in preparation for the dissociation phase of the experiment. The test cell was transferred to a walk-in freezer, depressurized, and subsequently opened to ensure that no bulk hydrate was present outside of the soil medium. During this period, the hydrated soil sample was maintained at atmospheric pressure and negative temperatures. Under these conditions, samples may be handled for periods of up to several hours without appreciable dissociation of gas hydrate. Known as "self-preservation" (Ershov and Yakushev, 1992), this metastable behavior is thought to be due to a protective ice shell that forms on gas hydrate surfaces following depressurization, thereby retarding further dissociation of the encased gas hydrate. Polyvinyl chloride (PVC) inserts were installed at this time to reduce the internal volume of the cell, allowing cell pressure to be increased more efficiently in response to a given amount of devolved gas. This facilitated the controlled dissociation of gas hydrate over a wider temperature range than would otherwise have been possible. The cell was repressurized to approximately 5 MPa, and cell temperature was increased to 1°C to promote reformation of the gas hydrate dissociated during depressurization and opening of the cell, after which the cell was again cooled to -3°C to freeze remaining sample water. The pressure within the cell was reduced slowly to a value just below that expected for methane hydrate stability (about 2.2 MPa). As cell temperature was gradually increased towards a target of 0°C, progressive dissociation of hydrate released additional methane gas into the free-gas space of the cell. Cell pressure continued to increase until an equilibrium condition was achieved (i.e. no further net dissociation), at which time pressure and temperature measurements were recorded. Cell temperature was subsequently raised in 0.5°C increments, with pressure and temperature conditions for methane hydrate stability recorded at each interval once equilibrium was achieved. This procedure was followed until all methane hydrate had completely dissociated, after which further increases in cell pressure were related solely to increases in temperature. Temperature measurements in these experiments are considered to be accurate within ± 0.1°C, and pressure readings within 0.1 MPa.

Samples 2, 3, and 4

It was anticipated that the test procedures utilized for sample 1 could not be effectively applied to test samples 2 through 4, due to the reduced amounts of methane hydrate expected in these sediments as a consequence of their elevated salt concentrations and/or grain-size influences. For samples containing substantially reduced amounts of gas hydrate, it was assumed that insufficient methane gas would be devolved upon dissociation to achieve equilibrium conditions over an extended temperature range. For samples 2 through 4, P-T conditions for methane hydrate stability were obtained by determining the point in time at which dissociation of hydrate was initiated during warming of the test cell. The gas charge within the test cell was adjusted prior to each new dissociation cycle, in order to achieve the desired distribution of P-T points over the temperature range of interest. The determination of a single P-T point using this procedure typically required 2–3 days. The dissociation point is characterized by a reduction in the rate of increase in sample temperature relative to that of the test cell and free-gas volume, as a consequence of the endothermic heat of hydrate dissociation within the sample. The temperature of the sample and the pressure existing within the test cell at this point in time are considered to identify the P-T 'threshold' for methane hydrate stability within the test sample.

RESULTS AND DISCUSSION

Pressure-temperature thresholds for methane hydrate stability in test samples

A critical aspect of the experiments described in this paper is the accuracy and character of the dissociation phase of each experiment. Pressure-temperature stability thresholds in sands containing substantial gas hydrate were determined through progressive dissociation. For saline and/or fine-grained sediments with relatively low concentrations of gas hydrate, we have found that the most reproducible method for establishing the dissociation point is to determine the point at which the temperature response of the sample deviates from that of the test cell during temperature-forced dissociation (stage D in Fig. 3). This deviation is assumed to result from endothermic cooling during initiation of gas hydrate dissociation within the sample, and thus identifies the P-T stability threshold. As shown in Figure 4 the trends for the sand samples and the silt samples have distinctly different characters. In general, temperature versus time plots for the sand samples showed a single, strong deviation in temperature that persisted for several hours (Fig. 4a). However, for the silt sample there was a lag response with an initial, very weak (primary) dissociation phase followed by a more vigorous secondary dissociation phase (Fig. 4b). This distinctive temperature

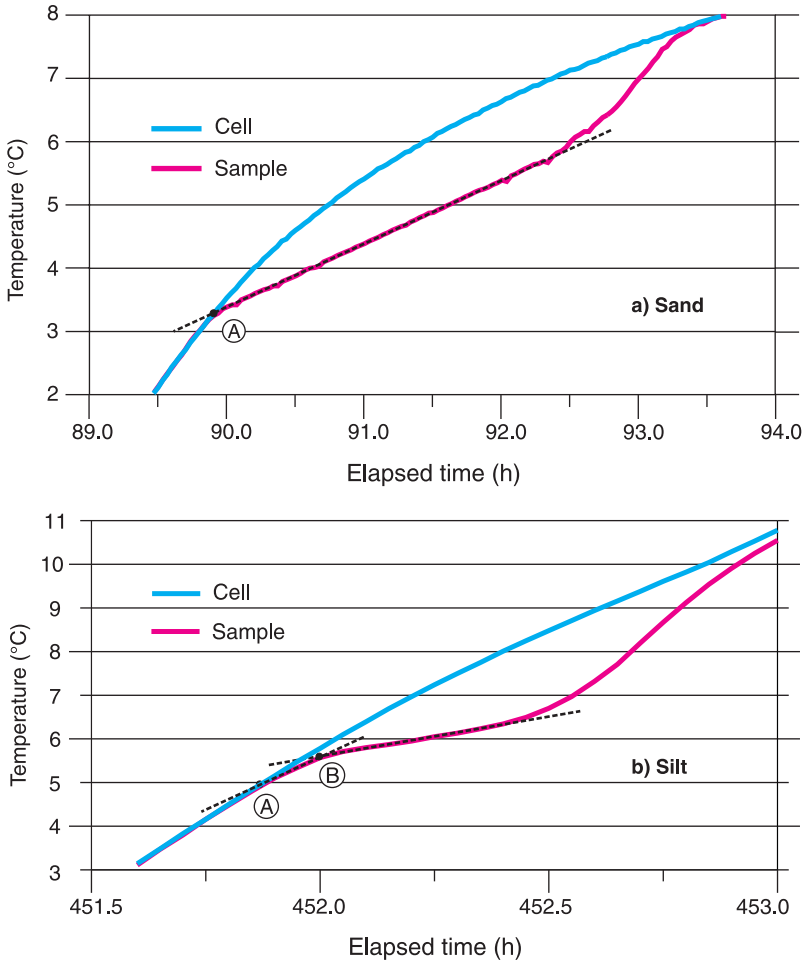

Figure 4.

Plot of test cell and sample temperatures during the dissociation of methane hydrate. Pressure-temperature phase-equilibrium conditions are determined at the point of divergence of the sample temperature from the established trend (A), as a result of the endothermy of dissociation. Figure 3a illustrates the situation typical for sands, with a single divergence point being evident. For methane hydrate dissociation in silts (Fig. 3b), divergence at 'A' is weak, and is followed by a second, stronger divergence at 'B'. Point 'A' is considered to be associated with initial dissociation of gas hydrate in very small, connecting pores characteristic of fine-grained sediments. At point 'B', the bulk of the remaining pore-space hydrate begins to dissociate.

response was observed for all dissociation events recorded in the silt experiment, and is considered to be related to different pore-water energy states controlled by the bimodal pore-size distribution characteristic of Mallik 2L-38 silts (Katsube et al., 1999).

When plotted over the full range of temperature and pressure conditions it is possible to establish the effects of pore-water salinity in the sands and infer the effects of the silt content. Figure 5 plots pressure-temperature relations defining the phase-equilibrium conditions for methane hydrate stability as determined during the controlled dissociation stages of the four experiments. Exponential best fits of the data are shown as solid or dashed lines. The solid dots represent P-T data points describing phase equilibrium conditions for methane hydrate stability in Mallik 2L-38 sand with 4 ppt salt (sample 1). Pressure-temperature data points were extracted from continuous recordings of P-T conditions within the test cell, sampled at approximately 0.5°C intervals once equilibrium conditions had been established. The data for sample 1 are in good agreement with empirical data describing P-T conditions for methane hydrate stability in pure water-methane systems (Sloan, 1990). Transient sensor problems prevented the acquisition of reliable data at the 1°C set point. It is clear that pressure-temperature conditions for methane hydrate stability in Mallik 2L-38 sample 1 do not deviate substantially from those expected for pure water-methane systems. Given the absence of a significant silt component in the sample, we should expect a negligible influence of particle surface area on water energy states within the soil matrix. While the pore waters of sample 1 did contain some salt (about 4 ppt), no shift was observed from the methane hydrate phase equilibrium boundary determined for fresh water, suggesting that this low concentration of salt had no significant influence on P-T conditions for methane hydrate stability.

Phase equilibrium conditions for methane hydrate stability in Mallik 2L-38 sands containing saline pore water (sample 2: 20 ppt salt, sample 3: 40 ppt) suggest a distinct and progressive shift in P-T stability conditions as pore-water salt concentration increases (compared to that expected in pure gas-water systems). Pressure-temperature conditions for these samples are adequately described by exponential functions, as was the case for the low-salinity test sand (sample 1). At a pressure of 6.5 MPa, the phase equilibrium boundary for methane hydrate in the high salinity sand (40 ppt) is shifted by approximately -2.0°C. The shift associated with the moderately saline sand (20 ppt) is roughly half that amount. In general, a moderately larger shift was observed at lower temperatures and pressures than at higher P-T values. By interpolating between the curves for samples 2 and 3, we can predict the P-T shift expected for Mallik 2L-38 sands having salt concentrations comparable to seawater (~30 ppt). Our data suggest a shift of -1.5°C at 6.5 MPa, which is larger than

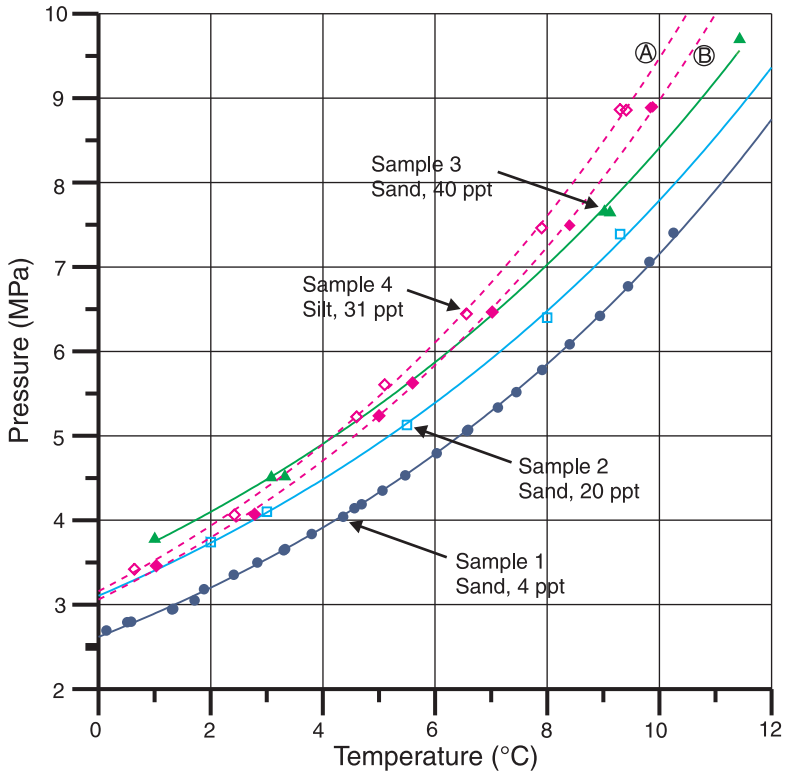

Figure 5.

Pressure-temperature stability thresholds determined for a variety of sediments recovered from the gas-hydrate-bearing zone at Mallik 2L-38. Note the nearly uniform shift in P-T stability conditions for saline sands over the temperature range of the plot. By contrast, for saline Mallik 2L-38 silt, a substantial shift observed at higher pressures and temperatures progressively decreases towards the low pressure, low temperature region of the plot. Primary and secondary dissociation thresholds for the silt sample tested are designated as 'A' and 'B' respectively (see also Fig. 4).

the value of -1.1°C determined for methane hydrate stability in seawater (Dickens and Quinby-Hunt, 1994) but in good agreement with the shift prediction by Englezos and Bishnoi (1988).

As was the case for the Mallik 2L-38 sands, P-T threshold conditions for the Mallik 2L-38 silt sample (sample 4: 31 ppt) may be described according to an exponential function (dashed lines, Fig. 5), with a shift offset from the pure system curve. Based on the P-T stability thresholds determined for saline sands, we should expect the P-T stability threshold for methane hydrate in sandy sediments (with 31 ppt salt) to be intermediate between the thresholds determined for samples 2 and 3. Interestingly, however, the shift is not uniform as was observed for the sands with different pore-water salinity. At relatively high temperatures and pressures, the observed shift in the P-T stability threshold is in excess of that attributed to salinity effects alone, and is assumed to result from the influences of particle surface area and pore-size characteristics of the fine-grained sediment (Fig. 5). The shift becomes progressively less as pressures and temperatures are reduced, until it has virtually disappeared at temperatures near 0°C. We have not yet developed a physical or thermodynamic model that adequately explains these observations, but planned future laboratory experiments using fine-grained materials (with and without the influence of salinity) are expected to clarify this issue.

Pore occupancy by gas hydrate

The volume of methane gas consumed during the gas hydrate formation stage (and thus, the amount of gas hydrate formed) was determined through analysis of the pressure-temperature-volume relations of the gas within the test cell. This calculation is straightforward (if the volume of the test cell and sample components are known) and provides reasonable estimates according to a comparison of calculated values and measurements of the volume of methane gas devolved from subsamples of gas-hydrate-bearing soils (Wright et al., 1999). In the current suite of experiments, calculations of methane consumption were made for the initial cycles of gas hydrate formation only (e.g. Fig. 3, for Mallik 2L-38 sample 2). Note that following the dissociation of all gas hydrate, cell pressure was about 7.7 MPa at hour 130, compared to an initial pressure of about 8 MPa at the start of the experiment. This difference is essentially a function of the pressure response to the lower cell temperature (12°C) relative to the initial temperature of about 22°C, and does not indicate a loss of the cell gas charge. The absence of system leaks was confirmed by returning the system to the initial temperature and comparing the resulting cell pressure to the initial pressure condition.

It was not possible to obtain a reliable estimate of methane consumption during the test on sample 4, due to an apparently nonlinearity of the relation between cell pressure and cell temperature during the initial cooling stage (observed in the fine-grained test sediment only). However, it is clear from the maximum pressure drop observed during gas hydrate formation in sample 4 that the amount of gas hydrate formed was very low in relation to samples 1 and 2, and probably less than was observed for sample 3.

Where the growth of gas hydrate progresses in saline sediments under a stable pressure and temperature regime, increases in pore-water salinity as a consequence of salt exclusion may eventually shift the P-T thresholds for gas hydrate stability to the extent that further growth of gas

Table 2. Pore-water characteristics following regrowth of methane hydrate in Mallik 2L-38 sediments.

Sample #	Class	Gravimetric water content (%)	Initial pore-water salinity (ppt)	Methane consumed: mL/g soil water*	% of water in gas hydrate structure	Gas hydrate pore occupancy (%)	Estimated salinity at end of GH** growth stage (ppt)
1	Sand	15.5	4	115	56	41	9
2	Sand	17.4	20	100	49	33	41
3	Sand	~17	40	16	8	6	43
4	Silt	12.5	31	n/a	<8	<6	31+

* Based on maximum methane consumption of 205 mL/g of water
** GH= gas hydrate
n/a= not available

hydrate is halted. In such a case, the increase in pore-water salinity limits the degree of pore occupancy by gas hydrate. For example, in Mallik 2L-38 sand with an initial salinity of 20 ppt (sample 2), gas hydrate growth rates decreased to insignificant levels following the incorporation of approximately 50% of water as hydrate. At this stage the salinity of the remaining pore water is estimated to have increased to about 41 ppt (Table 2) as a result of salt exclusion. This is comparable to the initial salinity of 40 ppt in sand sample 3, in which very low amounts of methane hydrate were formed. In both cases, limits to continued gas hydrate growth appear to have been associated with salinity values in excess of 40 ppt. However, the amount of gas hydrate formed prior to reaching this salinity threshold was much greater in sample 2 than in sample 3, and appears to be dependent upon the initial pore-water salinity of the sediments.

Therefore, we may expect gas hydrate concentrations to be very high in nonsaline, sandy sediments within the gas-hydrate-bearing interval, while adjacent fine-grained, saline sediments may contain no gas hydrate at all. According to well-log interpretations, gas hydrate concentrations at Mallik 2L-38 tend to be greatest in low salinity sands, while highly saline silt layers generally have low to very low concentrations (Fig. 6). Several sand samples of moderate to high salinity are located at transitions between highly saline silt layers and adjacent low-salinity sand deposits (e.g. at ~897 m; sample 2: 992.10 m), and appear to contain lower in situ concentrations of gas hydrate. Also note that the high-salinity sand layer between 893–895 m is interpreted as having very little in situ gas hydrate, however, it is unclear whether this is due to salinity effects alone, or a result of its location between two saline silt layers of relatively low permeability.

It should be noted that it is difficult to fully saturate natural sediments with gas hydrate in the laboratory. In experiments on nonsaline sands, this difficulty has been attributed primarily to the permeability characteristics of the porous medium, which limits the accessibility of soil pore water to sufficient quantities of methane gas within the relatively short time frames available. At present, therefore, we are unable to quantitatively separate the roles of permeability, grain-size influences, and salinity in limiting pore occupancy gas hydrate. Over geological time spans, the permeability characteristics of sediments are probably far less significant in determining the pore occupancy limits than is suggested by laboratory experiments. In natural settings, grain-size influences and pore-water salinity are probably the dominant factors limiting pore occupancy by gas hydrate.

Relevance to the geological situation at Mallik 2L-38

Location of the base of methane hydrate stability

The Mackenzie Bay and Kugmallit sequences, which make up the gas-hydrate-bearing interval at the Mallik site, consist of interbedded sands and silts. While there were no ground temperature measurements made at Mallik 2L-38 it is possible to constrain the in situ temperature conditions using local and regional ground temperature, heat flow, and permafrost data. According to extensive phase composition studies of core samples at negative temperatures and elevated pressures (*see* Taylor, 1999), the base of ice-bearing permafrost at Mallik 2L-38 is well defined at 640 m depth, with a corresponding temperature of -1°C. By extrapolating the regional geothermal gradient of 0.03°C/m (Judge and Bawden, 1987, p. 7) downward from the base of permafrost, we can predict that the theoretical base of methane hydrate stability for fresh water (and the low salinity sands tested in our laboratory) should occur at approximately 1135 m. Experimental results of P-T stability tests on saline Mallik 2L-38 sands indicate that P-T conditions for methane hydrate stability are shifted towards the high pressure–low temperature region, with this shift increasing as the pore-water salt concentration increases. Therefore, we should expect the base of methane hydrate stability in highly saline Mallik 2L-38 sands (e.g. sample 3: 40 ppt salt) to occur at approximately 1085 m (50 m above that expected for freshwater sands, Fig. 7). As described previously, P-T stability thresholds for the saline silt test sample indicate an enhanced shift at higher pressure and temperature conditions and a reduced shift at lower pressures and temperatures (relative to saline sand). At the pressures and temperatures occurring within the major gas hydrate accumulation at Mallik 2L-38, the base of methane hydrate stability in saline silts is inferred to occur at approximately 1025 m (110 m above that expected for freshwater sands; Fig. 7).

Direct correlation with the field situation is difficult because no core samples were taken below 1052 m. However excellent well-log data have allowed for comprehensive quantitative determinations of in situ gas hydrate contents and sediment characteristics (*see* Miyari et al., 1999; Collett et al., 1999). These determinations suggest that the deepest gas hydrate occurrence at Mallik 2L-38 is at 1106 m, within sands. Interpolating between points 'A' and 'B' in Figure 7, suggest that sands below this depth must have pore-water salinities greater than about 20 ppt, while the gas-hydrate-bearing sediments immediately above are likely to contain fresh or low-salinity pore water (<20 ppt). Our data suggest that where grain size is relatively uniform throughout a deposit, the internal variability in gas hydrate concentrations may be due entirely to effects of variable pore-water salinity. Certainly this situation was observed within the cored interval at Mallik 2L-38. We should note that well-log analysis techniques provide less reliable estimates of in situ gas hydrate concentrations in silt-rich sediments than in sands because of problems associated with the use of shale correction factors, and the lower gas hydrate contents within the silts in general (T.S. Collett, pers. comm, 1998). However, it is apparent that significant gas hydrate concentrations within silts are evident only within the upper portion of the gas-hydrate-bearing interval at Mallik 2L-38 (i.e. above 960 m depth).

Upper boundary for methane hydrate stability

At Mallik 2L-38, lower pressures and cooler temperatures exist at shallower depths in the sedimentary profile (Fig. 7). In fact, available information indicates that the stability zone extends well into the permafrost, and depending on salinity and grain-size influences, the upper boundary for methane hydrate stability at Mallik should be located between 200–300 m depth. The presence of natural gas hydrate within ice-bonded permafrost has been documented (Dallimore and Collett, 1995), and some evidence supports the existence of gas hydrate within permafrost at shallow depths, well outside of the accepted pressure-temperature stability envelope. Although no core samples were recovered between the base of permafrost and the top of the gas-hydrate-bearing zone,

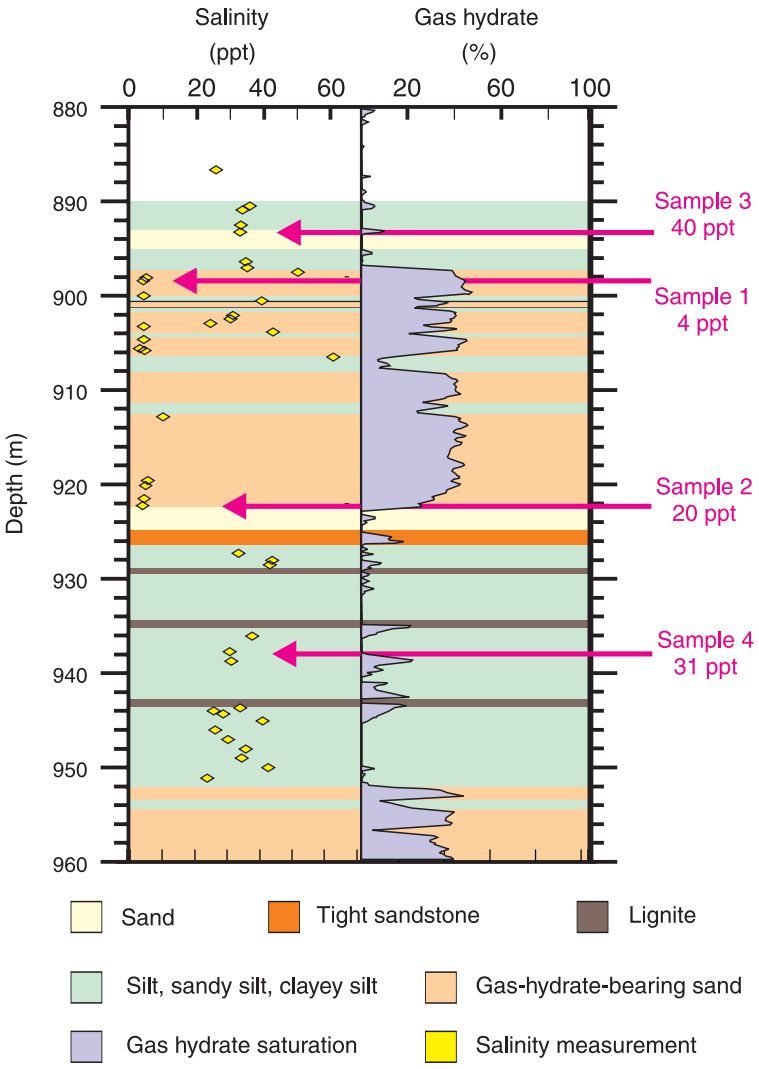

Figure 6.

Locations of Mallik 2L-38 test samples in relation to sediment layers within the upper portion of the gas-hydrate-bearing interval at Mallik 2L-38. The plot describes in situ gas hydrate concentrations (pore occupancy) in relation to sediment texture and measured in situ pore-water salinity.

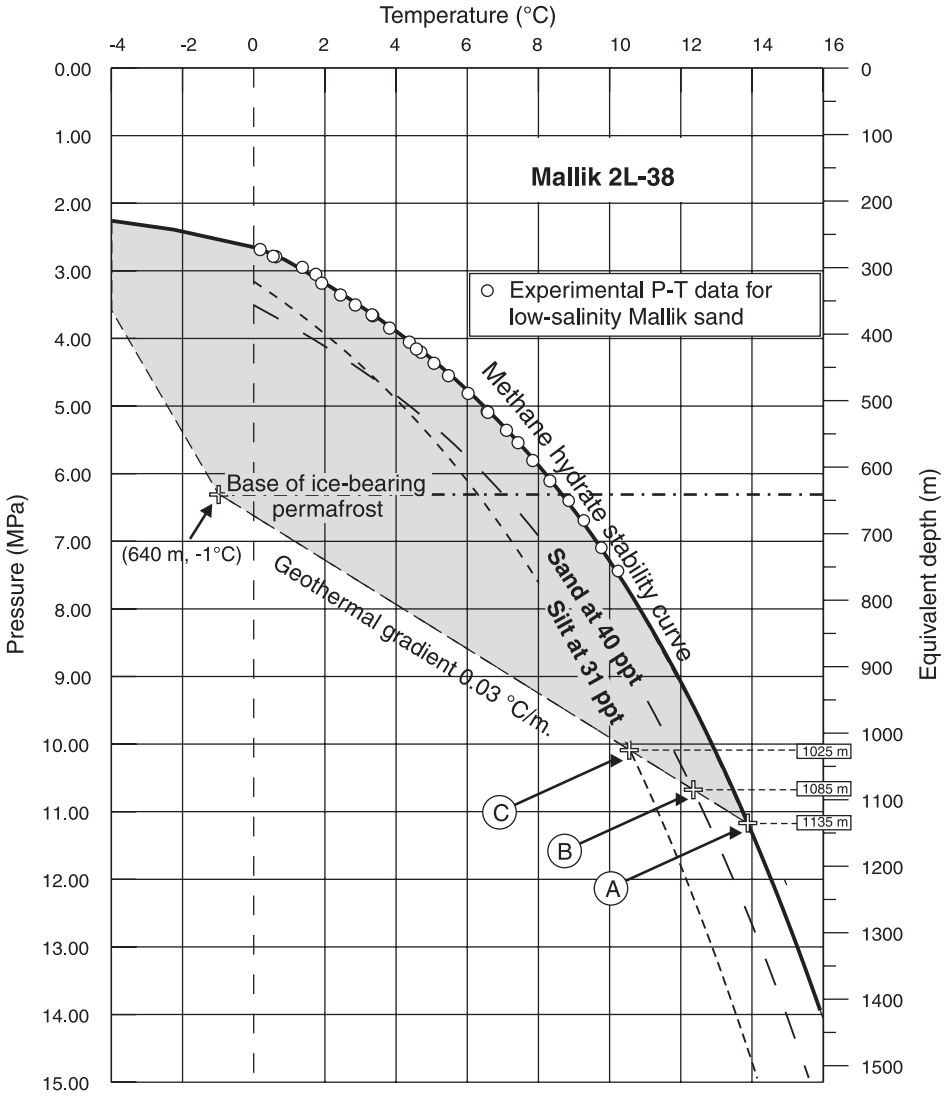

Figure 7. *Relations between the P-T stability thresholds determined for Mallik 2L-38 sands (4 ppt and 20 ppt pore-water salt concentration) and the location of the lower boundary of methane hydrate stability at Mallik 2L-38. Depths below ground surface are based on a pressure gradient of 0.0984 MPa/m (Bily and Dick, 1974). The intersection at 'A' and 'B' indicate the predicted base of methane hydrate stability for Mallik 2L-38 sands with pore-water salt concentrations of 4 ppt and 40 ppt respectively. The base of methane hydrate stability for Mallik 2L-38 silt (31 ppt salt) is predicted to occur at 'C'.*

well-log analysis confirms the absence of significant gas hydrate within this interval. Gas hydrate accumulation within this interval probably is limited by geological factors such as the supply of gas-hydrate-forming gases, the permeability characteristics of sediments (the presence of so-called 'seals' or 'caps'), and/or other influences, rather than by P-T conditions or the effects of salinity and grain size.

Our data suggest that at lower temperatures and pressures, P-T stability threshold in Mallik 2L-38 silt approach those observed in sand-dominated sediments. Such a possibility is supported to some extent by the experiments of Cha et al. (1988), in which enhanced methane hydrate stability was attributed to influences of the enclosing sediments (but in that case the sediments also contained a bentonite clay component). If such occurrences of shallow gas hydrates do exist, they must have persisted for very long periods of time, through mechanisms that are as yet only speculative. The lack of core recovery within the permafrost zone during drilling prevented the investigation of the possible occurrence of intrapermafrost gas hydrates at Mallik 2L-38. Considerable work remains before we can hope to determine the extent of

natural gas hydrate accumulations within the extensive permafrost regions, and to assess and evaluate its importance with respect to energy resource and climate change issues.

SUMMARY

The development of a simple gas hydrate test cell has facilitated laboratory investigations into P-T equilibrium thresholds for a variety of natural sediments collected from core samples recovered from the Mallik 2L-38 research well. Gas hydrate testing was carried out in two stages. Stage I involved the regrowth of methane hydrate in Mallik 2L-38 sediments with known physical properties and pore-water salinities. Stage II involved the determination of the pressure-temperature thresholds for methane hydrate stability in Mallik 2L-38 sediments, under controlled dissociation between 0°C and 12°C. For low-salinity sand, no discernible shift was apparent in the P-T equilibrium thresholds compared to published experimental data for methane hydrate formed from fresh water. Tests on saline sands indicate a substantial, but relatively uniform shift in P-T stability thresholds (compared to published values determined for seawater hydrate and freshwater hydrate) as pore-water salinity increases. Determination of the P-T stability threshold for a saline Mallik 2L-38 silt, suggest an additional shift in P-T stability conditions related to grain-size influences, but this shift becomes progressively smaller at lower pressures and temperatures, and is virtually absent near 0°C. Pore-water salinity and grain-size characteristics of host sediments are considered to have significant influences on natural gas hydrate occurrences in geological settings, including forcing shifts in P-T stability thresholds, and imposing limits on the degree of pore occupancy by gas hydrate.

ACKNOWLEDGMENTS

This work forms part of an ongoing gas hydrate research program at the Geological Survey of Canada. Financial support was provided by the Japanese National Oil Corporation (JNOC), the Japanese Petroleum Exploration Company (JAPEX), Natural Resources Canada's Panel on Energy Research and Development, and the Geological Survey of Canada. Testing was undertaken at the facilities of the Ottawa-Carleton Geocryology Research Laboratory. Technical support during development of the testing apparatus was provided by the Technical Services Branch at the Geological Survey of Canada and by Carleton University. Finally the authors would like to acknowledge their appreciation to the dedicated field staff who made possible the collection of the Mallik 2L-38 core samples.

REFERENCES

Bily, C. and Dick, J.W.L.
1974: Naturally occurring gas hydrates in the Mackenzie Delta, N.W.T.; Bulletin of Canadian Petroleum Geology, v. 22, no. 3, p. 340–352.

Cha, S.B., Oaur, H., Wildeman, T.R., and Sloan, E.D.
1988: A third surface effect on hydrate formation; Journal of Physical Chemistry, v. 92, p. 6492–6494.

Collett, T.S.
1993: Natural gas production from Arctic gas hydrates; *in* The Future of Energy Gases, (ed.) D.G. Howell; United States Geological Survey, Professional Paper 1570, p. 299–312.

Collett, T.S., Lewis, R., Dallimore, S.R., Lee, M.W., Mroz, T.H., and Uchida, T.
1999: Detailed evaluation of gas hydrate reservoir properties using JAPEX/JNOC/GSC Mallik 2L-38 gas hydrate research well downhole well-log displays; *in* Scientific Results from JAPEX/JNOC/GSC Mallik 2L-38 Gas Hydrate Research Well, Mackenzie Delta, Northwest Territories, Canada, (ed.) S.R. Dallimore, T. Uchida, and T.S. Collett; Geological Survey of Canada, Bulletin 544.

Dallimore, S.R. and Collett, T.S.
1995: Intrapermafrost gas hydrates from a deep core hole in the Mackenzie Delta, Northwest Territories, Canada; Geology, v. 23, no. 6, p. 527–530.
1998: Gas hydrates associated with deep permafrost in the Mackenzie Delta, N.W.T. Canada: Part I – Regional Overview; Proceedings of the 7th International Conference on Permafrost, Yellowknife, Northwest Territories, p. 201–206.

Dallimore, S.R., Collett, T.S., and Uchida, T.
1999: Overview of science program, JAPEX/JNOC/GSC Mallik 2L-38 gas hydrate research well; *in* Scientific Results from JAPEX/JNOC/GSC Mallik 2L-38 Gas Hydrate Research Well, Mackenzie Delta, Northwest Territories, Canada, (ed.) S.R. Dallimore, T. Uchida, and T.S. Collett; Geological Survey of Canada, Bulletin 544.

Dickens, G.R. and Quinby-Hunt, M.S.
1994: Methane hydrate stability in sea water; Geophysical Research Letters, v. 21, no. 19, p. 2115–2118.

Englezos, P. and Bishnoi, P.R.
1988: Predictions of gas hydrate formation conditions in aqueous electrolyte solutions; American Institute of Chemical Engineers, v. 34, p. 1718–1721.

Ershov, E.D. and Yakushev, V.S.
1992: Experimental research on gas hydrate decomposition in frozen rocks; Cold Regions Science and Technology, v. 20, p. 147–156.

Jenner, K.A., Dallimore, S.R., Clark, I.D., Paré, D., and Medioli, B.E.
1999: Sedimentology of gas hydrate host strata from the JAPEX/JNOC/GSC Mallik 2L-38 gas hydrate research well; *in* Scientific Results from JAPEX/JNOC/GSC Mallik 2L-38 Gas Hydrate Research Well, Mackenzie Delta, Northwest Territories, Canada, (ed.) S.R. Dallimore, T. Uchida, and T.S. Collett; Geological Survey of Canada, Bulletin 544.

Judge, A.S. and Bawden, W.
1987: Marine Science Atlas of the Beaufort Sea: Geology and Geophysics; (ed.) B.R. Pelltier; Geological Survey of Canada, Miscellaneous Report 40, p. 7.

Judge, A.S. and Majorowicz, J.A.
1992: Geothermal conditions for gas hydrate stability in the Beaufort–Mackenzie area: the global change aspect; Global and Planetary Change, v. 98, no. 2/3, p. 251–263.

Katsube, T.J., Dallimore, S.R., Uchida, T., Jenner, K.A., Collett, T.S., and Connel, S.
1999: Petrophysical environment of sediments hosting gas hydrate, JAPEX/JNOC/GSC Mallik 2L-38 gas hydrate research well; *in* Scientific Results from JAPEX/JNOC/GSC Mallik 2L-38 Gas Hydrate Research Well, Mackenzie Delta, Northwest Territories, Canada, (ed.) S.R. Dallimore, T. Uchida, and T.S. Collett; Geological Survey of Canada, Bulletin 544.

Lorenson, T.D., Whiticar, M., Waseda, A., Dallimore, S.R, and Collett, T.S.
1999: Gas composition and isotopic geochemistry of cuttings, core, and gas hydrate from the JAPEX/JNOC/GSC Mallik 2L-38 gas hydrate research well; *in* Scientific Results from JAPEX/JNOC/GSC Mallik 2L-38 Gas Hydrate Research Well, Mackenzie Delta, Northwest Territories, Canada, (ed.) S.R. Dallimore, T. Uchida, and T.S. Collett; Geological Survey of Canada, Bulletin 544.

Makogon, Y.F.
1981: Hydrates of Natural Gas; Penn Well Publishing Company, Tulsa, Oklahoma, 237 p.

Miyairi, M., Akihisa, K., Uchida, T., Collett, T.S., and Dallimore, S.R.
1999: Well-log interpretation of gas-hydrate-bearing formations in the Mallik 2L-38 gas hydrate research well; *in* Scientific Results from JAPEX/JNOC/GSC Mallik 2L-38 Gas Hydrate Research Well, Mackenzie Delta, Northwest Territories, Canada, (ed.) S.R. Dallimore, T. Uchida, and T.S. Collett; Geological Survey of Canada, Bulletin 544.

Sloan, E.D.
1990: Clathrate Hydrates of Natural Gases; Marcel Dekker, New York, 641 p.

Taylor, A.E.
1999: Modelling the thermal regime of permafrost and gas hydrate deposits to determine the impact of climate warming, Mallik field area; *in* Scientific Results from JAPEX/JNOC/GSC Mallik 2L-38 Gas Hydrate Research Well, Mackenzie Delta, Northwest Territories, Canada, (ed.) S.R. Dallimore, T. Uchida, and T.S. Collett; Geological Survey of Canada, Bulletin 544.

Uchida, T., Dallimore, S.R., Mikami, J., Nixon, F.M.
1999: Occurrences and X-ray computerized tomography (CT) observations of natural gas hydrate, JAPEX/JNOC/GSC Mallik 2L-38 gas hydrate research well; *in* Scientific Results from JAPEX/JNOC/GSC Mallik 2L-38 Gas Hydrate Research Well, Mackenzie Delta, Northwest Territories, Canada, (ed.) S.R. Dallimore, T. Uchida, and T.S. Collett; Geological Survey of Canada, Bulletin 544.

Winters, W.J., Dallimore, S.R., Collett, T.S., Katsube, J.T., Jenner, K.A., Cranston, R.E., Wright, J.F., Nixon, F.M., and Uchida, T.
1999: Physical properties of sediments from the JAPEX/JNOC/GSC Mallik 2L-38 gas hydrate research well; *in* Scientific Results from JAPEX/JNOC/GSC Mallik 2L-38 Gas Hydrate Research Well, Mackenzie Delta, Northwest Territories, Canada, (ed.) S.R. Dallimore, T. Uchida, and T.S. Collett; Geological Survey of Canada, Bulletin 544.

Wright, J.F., Chuvilin, E.M., Dallimore, S.R., Yakushev, V.S., and Nixon, F.M.
1999: Methane hydrate formation and dissociation in fine sands at temperatures near 0°C; *in* Proceedings of the 7th International Conference on Permafrost, Yellowknife, Northwest Territories, June 23–27, 1998, p. 1147–1153.

Yakushev, V.S. and Collett, T.S.
1992: Gas hydrates in Arctic regions: risk to drilling and production; *in* Proceedings of the Second International Offshore and Polar Engineering Conference, San Francisco, California, p. 669–673.